JASS 2008 - Joint Advanced Student School, Saint Petersburg, 9. - 19.3.2008
Modelling and Simulation in Multidisciplinary Engineering

Compressible Flows with Condensation and Cavitation - Modelling and Computation of Dynamic Phase Transition of Vapour and Liquids

Mihatsch M.
Technische Universität München,
Lehrstuhl für Fluidmechanik – Fachgebiet Gasdynamik,
D-85747 Garching Germany

Content

Abstract

This paper provides a small overview of unique aspects of compressible flows with condensation and cavitation. First, the effects of heat addition due to condensation are briefly discussed for a 2-D nozzle flow as well as for the flow through a cascade of a steam turbine. Furthermore, the difficulties of simulating cavitating liquid flows are explained and a modelling approach is presented. Finally, the resulting numerical approach **CATUM** (**C**avitation **T**echnische **U**niversität **M**ünchen) is validated by comparison of experimentally and numerically obtained results of an investigated 3-D cavitating liquid flow.

1 Introduction

Flows with dynamic phase transition are observed for a large variety of industrial applications. The design and optimization of thermal power plants enforce deep insight into the flow dynamics arising within steam turbines. Here, one observes the effects of condensation occurring in transonic flows of moist air or steam [1]-[7]. The presence of condensate is known to cause erosive effects due to impacting droplets on the surfaces of the blades. Furthermore, self excited oscillation leads to highly unsteady load as well as unsteady operating conditions of the turbine. Interestingly, one observes erosive effects as well as unsteady loads in water pumps and water turbines as well. However, the arising dynamic phase transition in those machines is no longer due to condensation of steam but it is due to evaporation -cavitation- of a liquid [8]-[12]. Typically, the evaporated liquid forms bubbles or bubble clusters (clouds) that are convected with the flow field until the surrounding static pressure compresses them, enforcing violent collapses that lead to the formation of erosive shocks and noise.
The paper therefore contains two major chapters: **Condensation** and **Cavitation**.

2 Condensation

Phase transition of vapor or vapor/carrier gas mixtures from the gaseous to the liquid phase occur close to equilibrium conditions **only** if the cooling rate is very small. This means that the time scales of the flow are much slower than the time scale of the phase transition process, for example as it is the case in the formation of clouds. **Figure 1** shows the Clausius-Clapeyron relation that resembles the equilibrium conditions -saturation conditions- of the pressure with respect to the temperature for a given fluid. Here, the solid black line separates the stable thermodynamic states of water vapor and liquid water. Contrary to the previously stated equilibrium condensation, this investigation focuses on non-equilibrium condensation arising within transonic flows with cooling rates of 10^6-10^7 K/s. Therefore, the time scale of the flow is faster than the time scale of the phase transition, which leads to subcooled vapor as sketched in **Fig. 1** – dotted red line. Now, nucleation and droplet growth (condensation) become significant and drive the meta-stable thermodynamic state towards the saturation line (stable equilibrium state). Thereby, the release of the latent heat occurs nearly instantaneous and leads to a significant alternation of the flow field. It is obvious that the heat addition to the remaining vapor or to the carrier gas can not be considered separately but has to be taken directly into account.

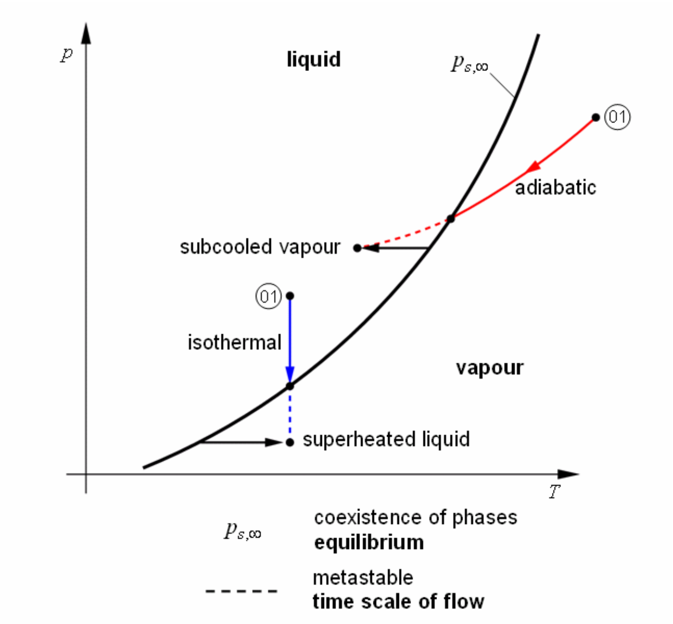

Figure 1: Pressure-temperature diagram showing the saturation curve of liquid and vapour. Cavitation (blue path) - Condensation (red path).

If the flow velocity is close to the speed of sound, just a small amount of heat addition already causes thermal choking. In constant area flows the maximum possible rate of heat addition that ensures that an initially stationary flow remains stationary depends on the undisturbed Mach number. It decreases and even vanishes if the Mach number becomes unity. If there is more heat released, the flow gets transient.

Figure 2 depicts Schlieren visualizations of a transient Laval nozzle flow of moist air. The grey scale corresponds to the gradient of the density in axial direction, where lighter areas indicate compressions while darker areas are rarefractions. The five pictures show five instants in time of one complete cycle of a self excited shock oscillation with a frequency of f_{cycle} = 950 Hz. Starting with the first picture, due to the strong acceleration and the corresponding static pressure drop through the nozzle, the vapour phase reaches a meta-stable state shortly after the nozzle throat.

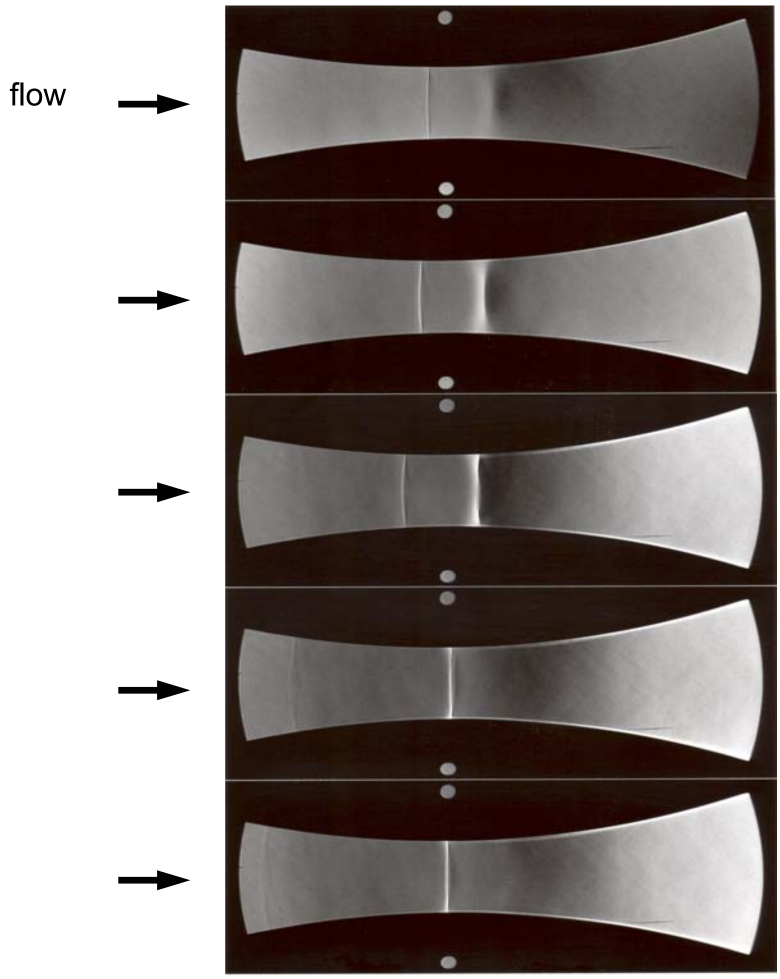

Figure 2: Schlieren visualization of self excited shock oscillation in a Laval nozzle.
Dots indicate the nozzle throat; circular arc nozzle, total throat height 30mm.

The release of latent heat caused by the onset of condensation causes a shock, displayed by the right bright line in the second picture. Here, the amount of heat released near the critical nozzle throat exceeds the possible amount of heat for a steady solution. Hence, the shock can not find a stable position and propagates upstream, even trough the nozzle throat (pictures 2-4). Thereby, the shock raises the temperature and the vapour phase behind the shock is no longer subcooled. Thus, condensation disappears (picture 5). With the shock disappearing upstream and the re-offset of the condensation process, the flow again accelerates to a velocity where the vapour phase reaches a meta-stable state and the next cycle starts (picture 1).

These fundamental mechanisms reach significant importance with respect to technical applications such as LP (Low Pressure) steam turbines. **Figure 3** shows the flow within two blades of a rotor cascade, flow direction is from the upper left to the lower right corner. The colour map depicts the average radius of the condensate droplets. The picture demonstrates that condensation takes place in the wake area, too. Due to the vortex shedding in this area and due to the low velocity of the wake, the average droplet radius strongly increases. In these pink coloured areas the average radius is nearly twice as large as in the surrounding flow field. From radius to the volume and finally to the momentum it can be estimated that these droplets hit the next stator cascade with eight times the impetus, resulting in vibration or even erosion.

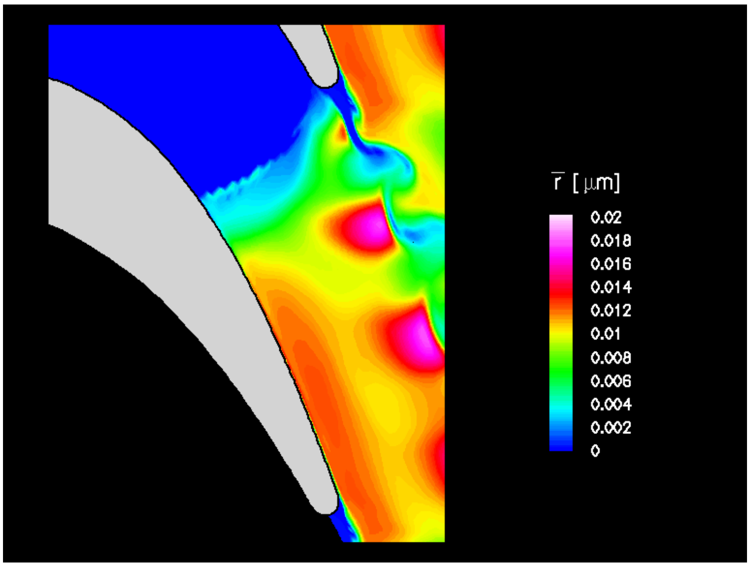

Figure 3: 2-D unsteady simulation of periodic droplet growth in the wake of a rotor of a LP steam turbine. The colour map corresponds to the local average droplet radius $\bar{r}$.

3 Cavitation

The significance of understanding cavitating flows is undoubtly related to its occurrence in various technical applications, such as hydraulic machinery and fuel injection systems, where due to the operating conditions cavitation is hardly avoidable. In these applications the instantaneous loads, caused by the collapse like recondensation of cavitation patterns, are one of the driving mechanisms of cavitation erosion. In order to highlight one basic erosion mechanism **Fig. 4** shows a sketch of a collapsing bubble at a wall [11]. The letters A to J correspond to subsequent instants in time but the time increments are strongly non-uniform. From a spherical collapse at the beginning until step C, a vertical flow direction becomes dominant starting around step E. The collapsing bubble deforms due to a micro jet, which is directed towards the wall. The impingement of the highly accelerated water jet at the wall (step J) produces pressure loads that are strong enough to cause erosion. This mechanism is directly related to the 'water hammer' or 'Joukowsky-shock'.

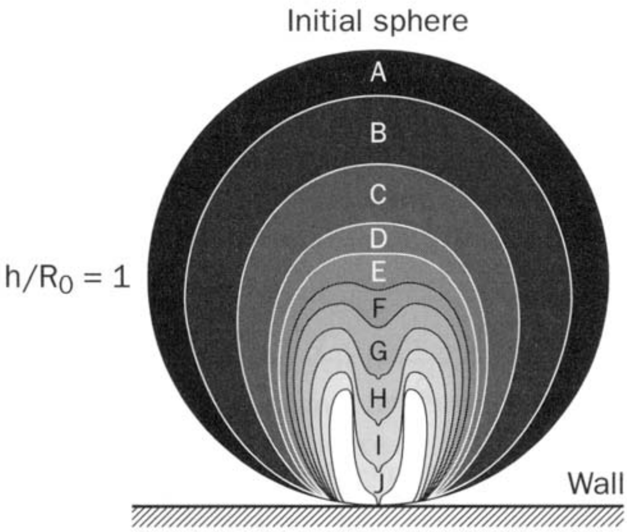

Figure 4: Sketch of the collapse mechanism and the jet formation of a cavitation bubble [11].

Both, modelling and the simulation of cavitation are rather challenging due to the huge variations of the density and of the speed of sound (strong nonlinear behaviour!). The coexistence of vapour and liquid within the same flow field implies density rations of the order of 10^5. In saturated mixtures, the speed of sound drops even below the values of the pure phases. In a saturated mixture of water and vapour the speed of sound drops to the order of 1 m/s, where it is approximately

1500 m/s in pure water. Thus the Mach number varies from values near to 0 in pure water to values of the magnitude of 10 in cavitating two phase areas within the same global flow field. Furthermore, the time steps of the simulation are linked to the smallest cell size and to the fastest signal speed. The reason therefore is the restriction that no information may travel trough more than one cell during one step. That means that the speed of sound of water divided by the simulation time step defines the smallest cell size that may be used within the computational grid. With respect to the required resolution to resolve cavitation structures the time step drops to the order of nanoseconds. The modelling of the two pure phases is achieved by the Tait-EOS for pure liquids and the ideal gas law for pure vapour. The two phase flow is modelled by a substitute fluid defined by the properties of a saturated mixture. Due to the dominance of inertia effects within the considered two phase flows, we neglect viscous effects and express the conservation principles by the Euler equations. However, the inclusion of dissipative mechanisms into the model is possible without restrictions.

These presumptions are justified by comparing a simulation result with an experiment. Therefore, we model and discretizise an experimental setup consisting of a rectangular test section, where a prismatic body is located at the bottom wall. The mesh consists of $3 \cdot 10^6$ finite volumes and the simulation requires a computational time of 240 hours using 64 processors for 10^6 time steps with a step size of $2.9 \cdot 10^{-7}$ s. That leads to a physical simulation time of 0.29 s. As shown in **Fig. 5**, the distribution of the simulated vapor volume fractions (void) match the experiment in detail.

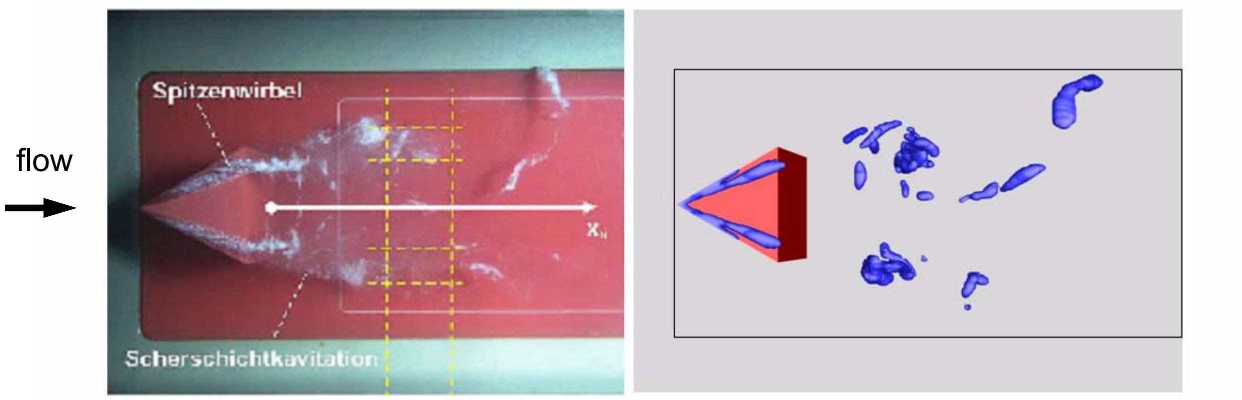

Figure 5: Top view of the prismatic body and the occurring cavitation structures - comparison of the experiment (left) to the numerical result (right).

The right picture is a time instant of the simulation, where the cavitation patterns are displayed by blue iso-surfaces of void fraction α= 0.1%. On the left side a picture of the experimental observation is shown. We observe weakly time dependent cavitating tip vortices at the top of the prismatic body, as well as highly unsteady cavitating vortices in the shear layer downstream. Furthermore, we detect the transition of the shape of cavitating patterns from compact clouds in the near wake to tube-like structures in the far wake. It can be seen that even manifold and complex shapes of the cavitation pattern are well predicted by the simulation.

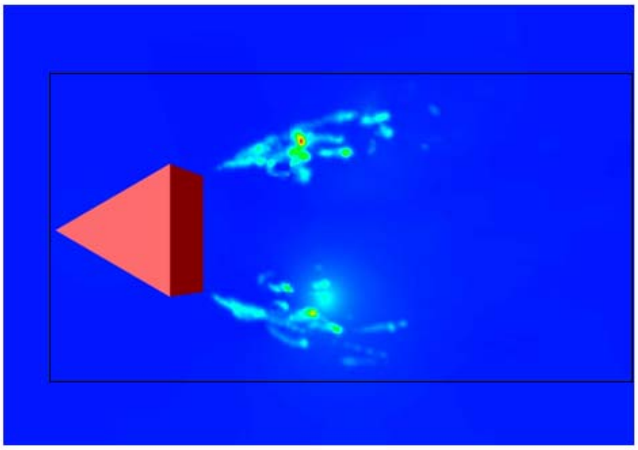

Figure 6: Top view of the prismatic body and the numerically obtained maximum pressure loads on the bottom wall, p_{max} = 70 bar.

The areas indicated by yellow lines in the left picture of **Fig. 5** are domains where intense erosion was experimentally observed. **Figure 6** shows a top view of the simulation, where the highest pressures at the bottom wall over the whole simulation time is displayed with a maximum pressure p_{max} = 70 bar. It shows that these areas match with the areas of intense erosion observed in the experiment. Thus we conclude that the CFD-Tool **CATUM** [12] is able to predict erosion sensitive areas within 3-D unsteady cavitating flows. With respect to the industrial relevance, the opportunity of predicting cavitation erosion enables design improvements of pumps or of ship propellers.

References (condensation and fundamentals of gas dynamics)

[1] Schnerr, G.H., Lecture notes on 'Gasdynamik', Technische Universität München, 2007.

[2] Schnerr, G.H., Lecture notes on 'Gasdynamische Strömungen mit Energiezufuhr und Phasenübergängen', Technische Universität München, 2007.

[3] Schnerr, G.H., 'Homogene Kondensation in stationären transsonischen Strömungen durch Lavaldüsen und um Profile', Habilitationsschrift, Karlsruhe, 1986.

[4] Schnerr, G.H., Adam, S., Mundinger, G., 'Selbsterregte Schwingungen in kompressiblen Zweiphasen-strömungen', Zeitschrift für angewandte Mathematik und Mechanik, Nr. 74, pp. 373-375 ,1994.

[5] Mundinger, G., 'Numerische Simulation instationärer Lavaldüsenströmungen mit Energiezufuhr durch homogene Kondensation', Ph.D. Thesis, Karlsruhe, 1994.

[6] Adam, S., Schnerr, G.H., 'Instabilities and bifurcation of non-equilibrium two-phase flows', Journal of Fluid Mechanics, vol. 348, pp.1-28, 1997.

[7] Heiler, M 'Instationäre Phänomene in homogen/heterogen kondensierenden Düsen- und Turbinenströmungen'. Ph.D. Thesis, Karlsruhe, 1999.

[8] Winkler, G., Schnerr, G.H. 'Nucleating Unsteady Flows in Low Pressure Steam Turbine Stages' Euroturbo 4, Firenze, Italy, pp. 793-802, 2001.

[9] Schnerr, G.H. 'Unsteadiness in condensing flow: Dynamics of internal flows with phase transition and application to turbomachinery', IMechE , vol. 219, Part C, pp. 1369-1410, 2005.

References (cavitation and CFD-Tool CATUM)

[8] Schnerr, G.H., Sezal, I.H., Schmidt S.J., 'Numerical investigation of 3-D cloud cavitation with special emphasis on collapse induced shock dynamics', Physics of Fluids, vol. 20, issue 4, 2008.

[9] Schmidt, S.J., Sezal I.H., Schnerr, G.H., Thalhamer M., 'Riemann Technique for the Simulation of Compressible Liquid Flows with Phase-transition at all Mach numbers – Shock and Wave Dynamics in Cavitating 3-D Micro and Macro Systems', 46th AIAA Aerospace Sciences Meeting and Exhibit, 7 - 10 January 2008, Reno, Nevada, USA, paper 2008-1238, 2008.

[10] Schmidt, S.J., Sezal I.H., Schnerr, G.H., Thalhamer M., 'Shock waves as driving Mechanism for Cavitation Erosion', Proc. 8th ISAIF - International Symposium on Experimental and Computational Aerothermodynamics of Internal Flows, Lyon, France, July 2-6, 2007 (eds. Ottavy, X., Trebinjac, I.), paper ISAIF8-0044, pp. 931-940, 2007.

[11] Plesset, M.S., Chapman, R.B., 'Collapse of an Initially Spherical Cavity in the Neighbourhood of a Solid Boundary', Journal of Fluid Mechanics, vol. 74, Issue 2, pp. 283-290, 1972.

[12] Further information about the CFD-Tool **CATUM**:http://www.lhm.mw.tu-muenchen.de/gd/